Reactive Flow of Magneto-Micropolar Fluid Along a Nonlinear Permeable Stretching Sheet in a Porous Medium.

E. O. Fatunmbi[1], S. O. Are[2]

[1-2]Department of Mathematics and Statistics, Federal Polytechnic, Ilaro, Nigeria.
E-mail: [1] olusojiephesus@yahoo.com, [2]stephen.are@federalpolyilaro.edu.ng
Corresponding e-mail: * olusojiephesus@yahoo.com

Abstract
The investigation of chemically reacting and electrically conducting micropolar fluid is numerically analyzed in this study. The flow is assumed to be two-dimensional, steady, incompressible and viscous along a nonlinear permeable stretching sheet in a saturated porous medium. The modelled equations are translated from partial to ordinary differential equations via a similarity conversion procedure and then integrated numerically by means of shooting technique in company of fourth order Runge-Kutta scheme. The numerical outcomes of the simulation are graphically displayed and the impact of the emerging controlling parameters on the fields of flow, temperature and concentration as well as quantities of engineering interest are discussed. A comparison of the present numerical results with existing data in literature as special cases depicts an excellent agreement. The results indicate that the mass transfer at the surface is boosted with growing magnitudes of first order chemical reaction parameter as the heat transfer also advances with a rise in nonlinear stretching parameter.
Keywords: Chemical reaction; micropolar fluid; nonlinear stretching sheet; porous medium

1 Introduction

The investigation of boundary layer flow and heat transfer prompted by stretching sheet has attracted researchers since initiated by Sakiadis (1961). Crane (1970) further worked on such problem owing to its wide industrial and engineering applications including the extrusion of plastic sheet, paper and textile production, hot rolling, wire drawing, etc. After the work of Crane (1970), quite a number of authors such as Gupta and Gupta (1977); Vajravelu and Nayfey (1993); Takhar *et al.* (1998); Chen and Char (1988); Mahmoud (2007); Kumar (2009); Fatunmbi and Fenuga (2017), etc have studied this problem with various parameters, geometries and methods. For the case of nonlinearly stretching sheet which often occur in practical situations,researchers such as Vajravelu (2001); Cortell (2007, 2008); Hayat (2008); Hsiao (2010); Alinejad and Samarbakhsk (2012); Ahmad *et al.* (2013); Rawat *et al.* (2016); Waqas *et al.* (2018); Fatunmbi *et al.* (2019), etc have reported such problem.
Eringen (1966) introduced the theory of micropolar which has the capacity to model and simulate complex and complicated fluid flow suc as liquid crystal, fluid with additives, animal blood etc. micropolar fluid is a non-Newtonian fluid with microstructures and rigid particles. They are significant in applications in diverse fields of engineering, science and technology such as in bio-medical engineering especially fluid flow in brains and blood flows also in metallurgical engineering and chemical engineering (Lukaszewicz, 1999; Reena and Rana, 2009; Rahman, 2009). Various scholars have examined different parameters on boundary layer flow with the use of micropolar fluid (see Kumar, 2009; Qasim ıet al., 2013; Mishra *et al.*, 2016; Mabood *et al.*, 2016; Fatunmbi and Adeniyan, 2018, Salawu and Fatunmbi, 2018).
However, these mentioned researches were conducted on the assumption that the no-slip boundary condition holds whereas in some practical situations, it has been found that this assumption becomes invalid. Hence, the need to investigate the influence of slip on both the

flow and heat transfer of fluids. Such study particularly important when studying particulate fluids such as emulsions and polymer solutions. Slip flow has been found to reduce flow resistance in micro-channels which is also connected with a rise in porous medium. It is also help in heat transfer processes including cooling of electronic devices, fuel cells and heat exchangers. Researchers such as Wang (2002); Hayat *et al.* (2010); Laxami and Shankar (2016); Awais (2016); Shu *et al.* (2017); Fatunmbi and Adeniyan (2018); Kumar *et al.* (2018); Mabood and Shateyi (2019). Meanwhile, these researches were conducted on a linearly stretching sheet ignoring cases when the stretching sheet is not linear.
In view of this, the objective of this study is to investigate hydromagnetic flow and heat transfer in micropolar fluid passing a nonlinear stretching sheet under the influence of thermal radiation, viscous dissipation, non-uniform heat source/sink, velocity and thermal slips. The wall heating condition has been assumed to be prescribed surface temperature, the governing equations are translated from partial to ordinary differential equations using similarity conversion approach and then solved via shooting and Runge-Kutta techniques.

2 Problem Formulation

Consider a two-dimensional, steady fluid flow over a non-linearly stretching permeable sheet in a saturated non-Darcian porous medium. The working fluid is an electrically conducting, incompressible, viscous micropolar fluid. A non-uniform magnetic field of strength $B(x) = B_0 x^{(r-1)/2}$ acts normal to the flow direction in which (x, y) describes the stretching and the transverse coordinates with corresponding velocity component (u, v) as depicted in Fig.1. The velocity of the stretching sheet in the x direction is u which varies in a nonlinear manner such that $u_w = bx^k$ with $b > 0$ being a constant and k is the power law index and u_s is the slip velocity, the surface temperature is taken as and surface concentration is taken as $C_w = C_\infty + D_1 x^{r_1}$ with r and r_1 representing the surface temperature and concentration parameters respectively.

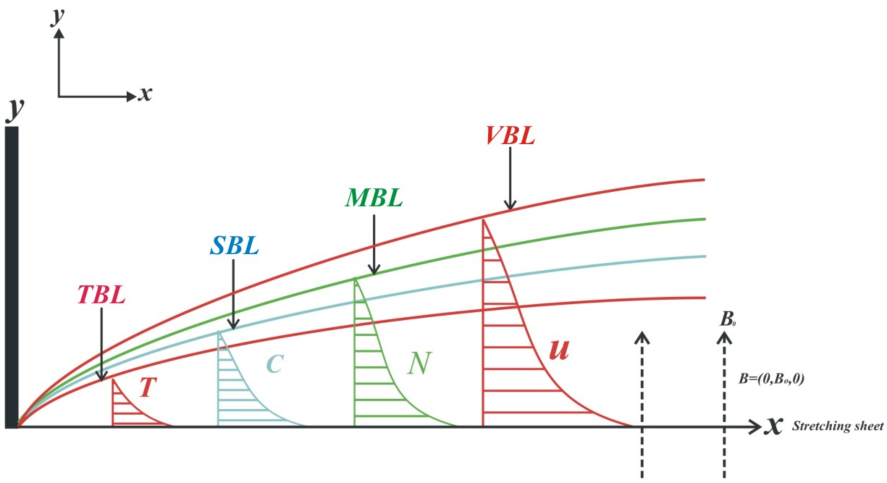

Fig.1. Flow Configuration and Coordinate System

With the above listed assumptions as well as the boundary layer approximations, the modelled governing boundary layer equations are:

$$\frac{\partial u}{\partial x} + \frac{\partial v}{\partial y} = 0, \tag{1}$$

$$u\frac{\partial u}{\partial x} + v\frac{\partial u}{\partial y} = \frac{1}{\rho_\infty}\left[\frac{\partial}{\partial y}(\mu\frac{\partial u}{\partial y}) + \kappa\frac{\partial^2 u}{\partial y^2}\right] + \frac{\kappa}{\rho_\infty}\frac{\partial B}{\partial y} - \left(\frac{\sigma B_0^2}{\rho_\infty} + \frac{(\mu+\kappa)}{\rho_\infty K_p}\right)u, \tag{2}$$

$$u\frac{\partial B}{\partial x} + v\frac{\partial B}{\partial y} = \frac{\gamma}{\rho_\infty j}\frac{\partial^2 B}{\partial y^2} - \frac{\kappa}{\rho_\infty j}\left(2B + \frac{\partial u}{\partial y}\right), \tag{3}$$

$$u\frac{\partial T}{\partial x}+v\frac{\partial T}{\partial y}=\frac{\zeta}{\rho_\infty C_p}\left(1+\frac{16T_\infty^3\sigma^\star}{3k^\star\zeta}\right)\frac{\partial^2 T}{\partial y^2}+\frac{(\mu+\kappa)}{\rho_\infty C_p}\left(\frac{\partial u}{\partial y}\right)^2+\frac{\sigma B_0^2}{\rho_\infty}C_p u^2, \tag{4}$$

$$u\frac{\partial C}{\partial x}+v\frac{\partial C}{\partial y}=Dm\frac{\partial^2 C}{\partial y^2}-k_r\left(C-C_\infty\right). \tag{5}$$

The wall conditions are:

$$\begin{aligned}&u=u_w=bx^k, v=V_w, B=-r\frac{\partial u}{\partial y}, T=T_w=T_\infty+D_1\left(\frac{x}{l}\right)^\alpha,\\ &C=C_w=C_\infty+D_2\left(\frac{x}{l}\right)^\beta \ \ at\ y=0,\\ &u\to 0, B\to 0, T\to T_\infty, T\to T_\infty \ \ \text{as} \ \ y.\end{aligned} \tag{6}$$

Following previous authors, the variation of the viscosity $\mu(T)$ with temperature is assumed to be inverse form expressed as is expressed as see (Kumari, 2001; Chin *et al.,*, 2007; Makinde, 2011).

$$\frac{1}{\mu}=\frac{1}{\mu_\infty}\left[1+N\left(T-T_\infty\right)\right]=G\left(T-T_r\right), \tag{7}$$

with

$$G=\frac{N}{\mu_\infty}, T_r=T_\infty-\frac{1}{N} \tag{8}$$

Table 1 shows the nomenclature of the symbols used in Eqs. (1-6).

Table 1: Nomenclature of the symbols in Eqs. (1-6)

Symbols	Nomenclature	Symbols	Nomenclature
μ	dynamic viscosity	ρ	density
κ	vortex viscosity	ν	kinematic viscosity
σ	electrical conductivity	T	temperature
α	surface Temp. Parameter	C	concentration
β	surface Conc. Parameter	Dm	mass diffusivity
k^*	mean absorption coefficient	$\sigma^\star$	Stefan-Boltzmann constant
u	velocity component in x	r	surface parameter
v	velocity component in y	$A\&D\&G$	constants
γ	spin gradient viscosity	V_w	suction/injection term
ζ	thermal conductivity	k_r	rate of chemical reaction
N	fluid thermal nature	T_r	constant

The governing Eqs. (1-6) are converted from to ODEs using Eq. (8) (see Salem, 2013; Hayat, 2008)

$$\begin{aligned}&\eta=y\left[\frac{b(k+1)x^k}{2x\nu_\infty}\right]^{1/2}, u=cx^kf', v=-\left[\frac{b\nu_\infty(k+1)}{2}\right]^{1/2}x^{(k-1)/2}\left(f+\frac{(k-1)}{(k+1)}\eta f'\right),\\ &B=x^{(3k-1)/2}\left[\frac{b^3(k+1)}{2\nu_\infty}\right]^{1/2}h(\eta), \gamma=\left(\mu+\frac{\kappa}{2}\right)j, \phi(\eta)=\frac{C-C_\infty}{C_w-C_\infty},\\ &\theta(\eta)=\frac{T-T_\infty}{T_w-T_\infty},\ j=\left(\frac{\nu_\infty}{b}\right)x^{(1-k)}.\end{aligned} \tag{9}$$

Using Eq. (8) in Eqs. (2)-(5) result to:

$$\left(\frac{Qr}{Qr-\theta}+L\right)f'''+ff''+Lh'-\frac{Qr}{(Qr-\theta)^2}\theta'f''-\left(\frac{2k}{k+1}\right)f'^2-\left(\frac{2}{k+1}\right)\left[M+Da\left(\frac{Qr}{Qr-\theta}+L\right)\right]f'=0, \tag{10}$$

$$\left(1+L/2\right)h''+fh'-\left(\frac{3k-1}{k+1}\right)f'h-L\left(2h+f''\right)\left(\frac{2}{k+1}\right)=0, \tag{11}$$

$$\begin{aligned}&\theta''+Prf\theta'-\left(\frac{2\alpha}{k+1}\right)Prf'\theta+\left(\frac{Qr}{Qr-\theta}+L\right)PrEcx^{2k-r}f''^{2}+\\&\left(\frac{2}{k+1}\right)MPrEcx^{2k-r}f'^{2}=0,\end{aligned} \tag{12}$$

On setting $\alpha=2k$, Eq. (10) becomes

$$(1+Nr)\theta''+Pr\left[f\theta'-\left(\frac{4k}{k+1}\right)f'\theta\right]+\left(\frac{Qr}{Qr-\theta}+L\right)PrEcf''^{2}+\left(\frac{2}{k+1}\right)MPrEcf'^{2}=0. \tag{13}$$

$$\phi''+Scf\phi'-\left(\frac{2\beta}{k+1}\right)Sc\phi f'-\left(\frac{2}{k+1}\right)ScK\phi=0, \tag{14}$$

and the boundary conditions translate to

$$\begin{aligned}&\eta=0: f'=1,\ f=Fw,\ h=-rf'',\ \theta=1,\phi=1\\&\eta\to\infty: f'\to 0\ h\to 0,\ \theta\to 0,\phi\to 0.\end{aligned} \tag{15}$$

Where $L=\frac{\kappa}{\mu_\infty}$ is the micropolar material parameter, $Fw=\frac{-\sqrt{2}V_0}{\left(\sqrt{b\nu_\infty(n+1)}\right)}$ stands for the suction/injection parameter with $Fw>0$ represents injection and $Fw<0$ corresponds to injection. $M=\frac{\sigma B_o^2}{b\rho_\infty}$ is the Magnetic parameter, $Pr=\frac{\mu_\infty Cp}{\zeta}$ is the Prandtl number, $Ec=\frac{b^2x^{2n}}{C_p(T_w-T_\infty)}$ is the Eckert number, Sc is the Schmidt number, K is the chemical reaction parameter.

For the current work the quantities of engineering interest are the skin friction coefficient C_{fx}, Nusselt number Nu_x and Sherwood number Sh_x defined respectively as.

$$C_{fx}=\frac{\tau_w}{\rho u_w^2},Nu_x=\frac{xq_w}{k\left(T_w-T_\infty\right)},Sh_x=\frac{xq_m}{D_m\left(C_w-C_\infty\right)}, \tag{16}$$

with

$$\tau_w=\left[\left(\mu+\kappa\right)\frac{\partial u}{\partial y}+\kappa B\right]_{y=0},\ q_w=-\left[\left(\zeta+\frac{16T_\infty^3\sigma^\star}{3k}\right)\frac{\partial T}{\partial y}\right]_{y=0},q_m=-\left(Dm\frac{\partial C}{\partial y}\right)_{y=0}, \tag{17}$$

where τ_w is surface shear stress, q_w, q_m is surface heat and mass flux in that order. Using equations (8) and (16), the dimensionless skin friction coefficient is

$$C_{fx}=\left(\frac{n+1}{2}\right)^{1/2}\left[\frac{Qr}{Qr-\theta}+\left(1-s\right)L\right]Re_x^{-1/2}f''(0), \tag{18}$$

the Nusselt and Sherwood numbers respectively translate to

$$Nu_x=-\left(1+Nr\right)\left(\frac{n+1}{2}\right)^{1/2}Re_x^{1/2}\theta'(0),Sh_x=-\left(\frac{n+1}{2}\right)^{1/2}Re_x^{1/2}\phi'(0) \tag{19}$$

3 Validation of Results

Owing to the highly nonlinearity of the governing equations, the present study has been solved numerically by means of shooting technique in company of Runge-kutta order four.

The validity of the numerical code has been checked by direct comparison of the computational values gotten in this study with earlier reported related studies in literature in the limiting cases. Table 1 shows the computed values of the skin friction coefficient C_{fx} as compared with those of Mabood & Das (2016) for variation in M via implicit finite difference method with quasilinearisation technique when $n = 1,\ K = fw = Ec = Pr = L = Q = 0$. Also, for variation in the non-linear stretching parameter n comparison of C_{fx} values has been made with those reported by Hayat *et al.* (2008) via HAM when $K = L = Q = M = fw = 0$.

Table 1: Computational values of C_{fx} as compared with published works

M	Mabood & Das (2016)	Present	n	Hayat et al. (2008)	Present
0.0	1.000008	1.000008	0.0	0.627555	0.627555
1.0	1.4142135	1.4142135	0.2	0.766837	0.766837
5.0	2.4494897	2.4494897	0.5	0.889544	0.889544
10.0	3.3166247	3.3166247	1.0	1.000000	1.000008
50.0	7.1414284	7.1414284	1.5	1.061601	1.061601
100.0	10.049875	10.049875	3.0	1.148593	1.148593
500.0	22.383029	22.383029	7.0	1.216850	1.216850
			10.0	1.234875	1.234875
			20.0	1.257424	1.257424
			100.0	1.276774	1.276774

In addition, we have also cross-checked the values of the Nusselt number obtained in this study with those reported by Ali (1994) and Mabood & Shateyi (2019) for variation in the Prandtl number Pr for isothermal situation, linearly stretching sheet $n = 1$ and when $M = fw = Ec = \alpha = \beta = Q = K = 0$. These are recorded in Table 2 and shows that the results gotten from the current work compare favourably with the published articles in the limiting cases.

Table 2: Computational values of Nu_x for variation in Pr

Pr	Ali (1994)	Mabood & Shateyi (2019)	Present
0.72	0.8058	0.8088	0.80883
1.0	0.9691	1.0000	1.00000
3.0	1.9144	1.9237	1.92369
10.0	3.7006	3.7207	3.72067

4 Results Analysis and Discussion

The reaction of the dimensionless velocity, microrotation, temperature to variation in the physical parameters have been analyzed through various graphs. Also, the impact of some of these parameters on the skin friction coefficient C_{fx} and Nusselt number Nu_x have been found. The default values used for the computational analysis have been carefully chosen from existing works in literature that are found suitable. These values are $K = s = 0.5, Ec = 0.1, n = 0.5, Sc = 0.22, fw = 0.3, M = 0.5, Pr = 0.71, \alpha = L = Q = 0.3, \beta = 0.1$. Unless otherwise stated on the graphs.

The plot in Fig. 2 shows that the micropolar fluid represented by K has the tendency to boost the fluid velocity whereas the effect of magnetic field parameter is to lower the fluid motion due the introduction of Lorentz force. The exact of opposite of the trend in Fig. 2 happens in Fig. 3 where as a result of the presence of micro particles, the microrotation field reduces. However, the magnetic field parameter M acts to favour the growth of the microrotation field.

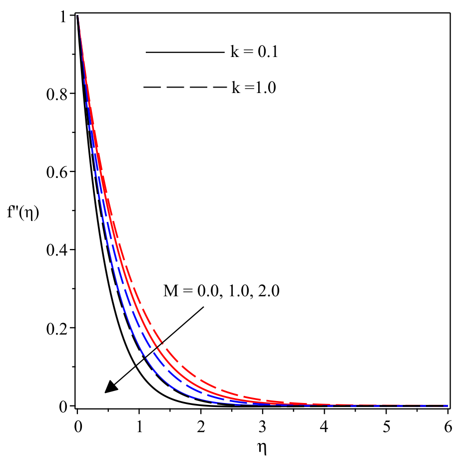

Fig. 2 Impact of $K\&M$ on velocity field

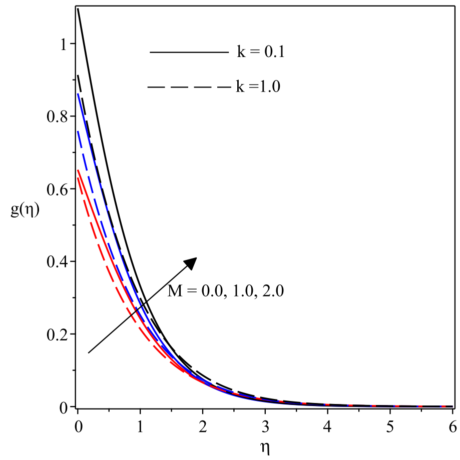

Fig. 3 Variation of $K\&M$ on microrotation field

The plot representing the velocity field against η as the velocity slip parameter L varies is depicted in Fig. 4. Observation shows that the impact of L is to decrease the momentum boundary layer which in turn act to reduce the locomotion of the fluid. A situation of no-slip $L = 0$ offers higher fluid flow than the presence of slip condition. Similarly, the variation of the temperature profiles with thermal slip term also informs that the thermal boundary layer thickness thins out as Q rises in magnitude. In view of this, there is a low rate of heat transfer from the nonlinear stretching sheet to the fluid, an observation which agrees well with the report Ramya et al. (2018).

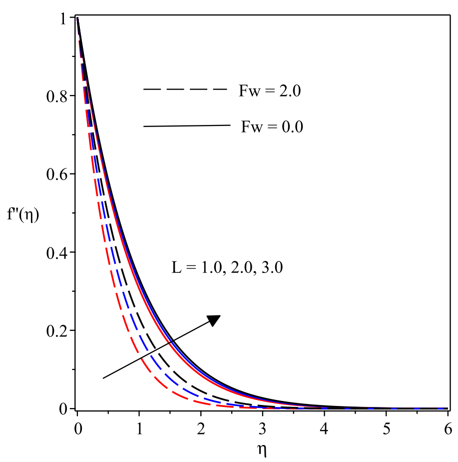

Fig. 4 Response of velocity profiles with L

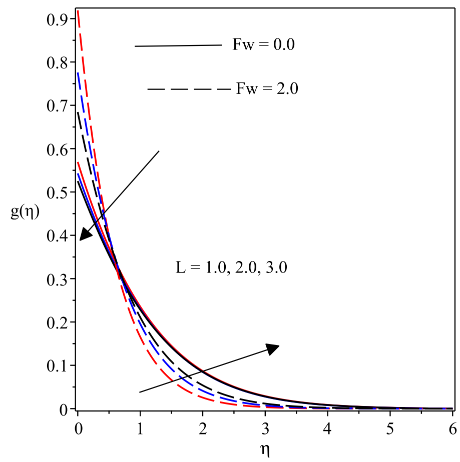

Fig. 5 Reaction of temperature field with Q

Fig. 6-7 depict the influence of the nonlinear stretching parameter n on the velocity and thermal fields respectively in the presence and absence of of the magnetic field parameter. Clearly, the fluid flow declines with an increase in n in the absence of M i.e. $M = 0$. However, with the introduction of M, the motion of the fluid rises as n is increasing. In Fig. 7, the temperature declines for both situations, however, the temperature is higher in the presence of M, i.e. $M = 0.5$.

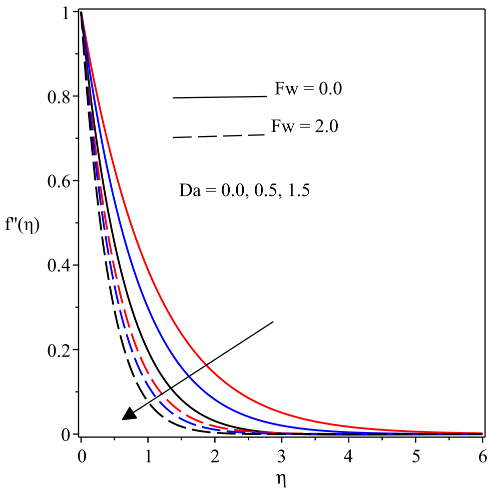

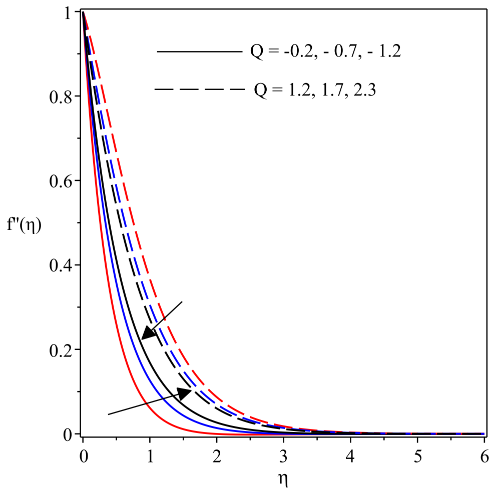

Fig. 6 Effect of n & M on velocity **Fig. 7** Effect of n & M on temperature field

The sketch in Fig. 8 describes the effects of the Prandtl number and space-dependent heat source parameter α on the thermal field. It is revealed that the thermal boundary layer declines with rising values of Pr, hence, the drop in the surface temperature. Contrarily, the imposition of α provides more heating in the system thereby enhancing the temperature profiles. In the same vein, the thermal field is enhanced with the imposition of the temperature-dependent heat source parameter β as depicted in Fig. 9.

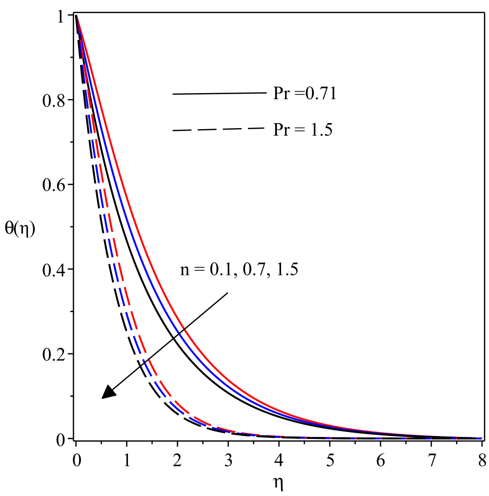

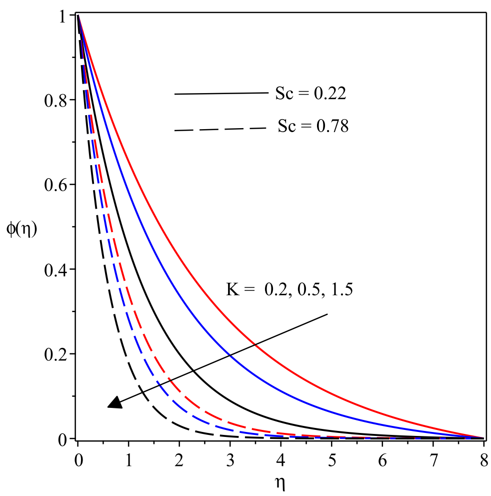

Fig. 8 Variation of temperature with Pr & α **Fig. 9** Display of β on temperature field

Fig. 10 shows that for any value of the magnetic field term, the micropolar fluid reduces the skin friction coefficient C_{fx} whereas an increase in M boosts C_{fx}. On the other hand, an increase in M turns to lower the rate of heat transfer at the surface as seen in Fig. 11 while the impact of micropolar term k is to facilitate the Nusselt number.

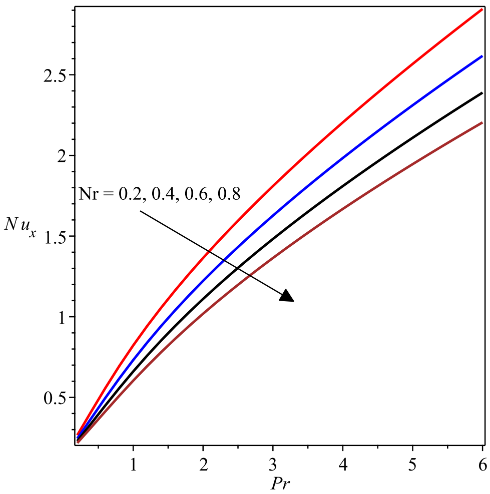

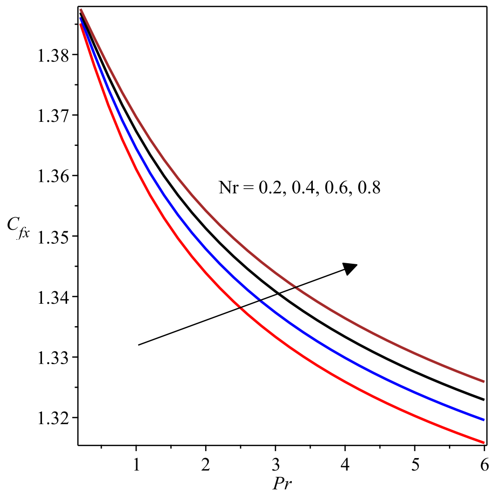

Fig. 10 Variation of C_{fx} with $M\&K$ **Fig. 11** Response of Nu_x with varying $M\&K$

Fig. 12 is graph of variation of the Nusselt number with the Prandtl number in the presence of viscous dissipation term known as Eckert number Ec. The heat transfer at the sheet surface declines with a rise in Ec. However for a fixed value of Ec, an increase in Pr boosts the transfer of heat. The reaction of Nusselt number with changes that occur in Pr in the presence of nonlinear stretching parameter n and for the presence and absence of heat source parameters α/β are plotted in Fig. 13. The transfer of heat is facilitated with rising values of n for both presence and absence of heat source parameter, this response is in line with the report of Ahmad *et al.* (2013). With the stretching of the sheet, the values of the Nusselt number rises for a particular value on n. However, the value of Nusselt number Nu_x is higher in the absence of heat source parameter α/β.

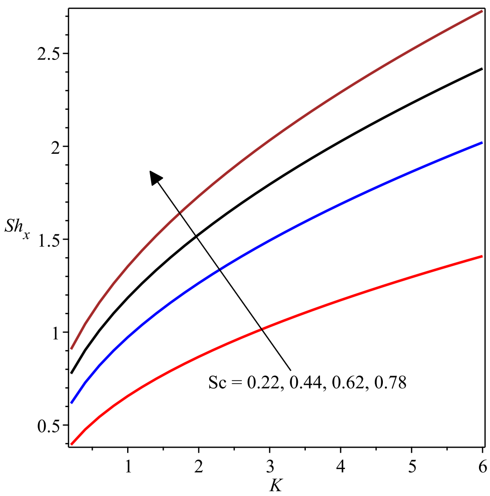

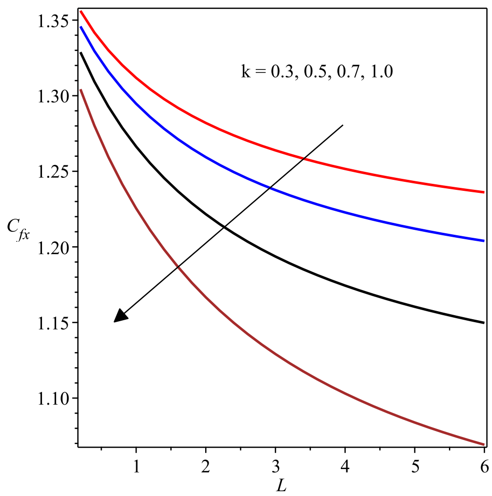

Fig. 12 Impact of $Ec\&Pr$ on Nu_x **Fig. 13** Reaction of $n\&\alpha/\beta$ on Nu_x

5 Conclusion

The current study has addressed hydromagnetic flow of micropolar fluid along a nonlinear stretching sheet under the influence of nonuniform heat source/sink, viscous dissipation, velocity and temperature slip conditions. The dimensionless equations of the flow and heat transfer have been solve numerically using the shooting techniques and Runge-Kutta scheme. Also, validation of the results obtained was carried out with existing data in literature in the limiting cases and found to be in good relationship. Moreso, the effects of main controlling parameters have been analyzed by means of various graphs. From this study, the following points have been noticed

- The transfer of heat at the sheet surface is boosted with increasing values of the nonlinear stretching parameter n, Prandtl number Pr and micropolar parameter K while it declines with rising values of the magnetic field M and Eckert number Ec parameters.

- The fluid motion is enhanced in the presence of micropolar parameter K whereas the presence of the magnetic field parameter M inhibits the fluid flow.

- The hydrodynamic boundary layer becomes thin in the presence of slip parameter L as the the thermal boundary layer also falls in the presence of temperature slip parameter Q. Hence both velocity and temperature profiles depreciate with a rise in the slip parameters.

- There is a drop in the surface temperature with rising values of the nonlinear stretching parameter n, Prandtl number Pr whereas the imposition of heat source enhances the temperature field.

References

Ahmad, K., Ishak, A and Nazar, R. (2013). Micropolar fluid flow and heat transfer over a nonlinearly stretching plate with viscous dissipation. *Mathematical Problems in Engineering, 2013*, 1-5.

Ali, M. E. (1994). Heat transfer characteristics of a continuous stretching surface. ıWarme- und Stoffubertragung, 29(4), 227–234.

Alinejad, J. and Samarbakhsh, S. (2012). Viscous flow over nonlinearly stretching sheet with effects of viscous dissipation. *Journal of Applied Mathematics, 2012*, 1-10.

Cortell, R, (2007). viscous flow and heat transfer over a nonlinearly stretching sheet, *Applied Mathematics and Computation 184*, 864–873.

Cortell, R. (2008). Effects of viscous dissipation and radiation on the thermal boundary layer over a nonlinearly stretching sheet. *Physics Letters A, 372*, 631-636.

Crane, L. J. (1970). Flow past a stretching plate. *Communicatios Breves, 21*, 645-647.

Eringen, A. C. (1966). Theory of micropolar fluids. *J. Math. Anal. Appl., 16*, 1-18.

Fatunmbi, E. O. and Fenuga, O. J. (2017). MHD micropolar fluid flow over a permeable stretching sheet in the presence of variable viscosity and thermal conductivity with Soret and Dufour effects. *International Journal of Mathematical Analysis and Optimization: Theory and Applications, 2017*, 211- 232.

Gupta, P. S. and Gupta, A. S. (1977). Heat and mass transfer on a stretching sheet with suction or blowing. *Can. J. Chem. Eng., 55*, 744-746.

Hayat, T. and Abbas, Z. and Javed, T. (2008), Mixed convection flow of a micropolar fluid over a non-linearly stretching sheet. *Physic Letter A*, 372, 637-647.

Hsiao, K. L. (2010). Heat and mass transfer for micropolar flow with radiation effect past a nonlinearly stretching sheet. *Heat Mass Transfer, 46*, 413-419.

Kumar, L. (2009). Finite element analysis of combined heat and mass transfer in hydromagnetic micropolar flow along a stretching sheet. *Comput Mater Sci, 46*, 841-848. Doi: 10.1371/journal.pone.0059393

Mabood, F and Shateyi, S. (2019). Multiple Slip Effects on MHD Unsteady Flow Heat and Mass Transfer Impinging on Permeable Stretching Sheet with Radiation. *Modelling and Simulation in Engineering, 2019*, 1-11, Doi.org/10.1155/2019/3052790

Mahmoud, M. A. A. (2012). Thermal radiation effects on MHD flow of a micropolar fluid over a stretching surface with variable thermal conductivity *Physica A , 375*, 401-410. doi:10.1016/j.physa.2006.09.010.

Qasim, M,, Khan, I. and Shafie, S. (2013). Heat transfer in a micropolar fluid over a stretching sheet with Newtonian heating. *Plos One, 2013*(4), 1-7.

Ramya, D., Chamkha, A. J., Srinivasacharya, R. and Rao, J. A. (2018). Effects of velocity and thermal wall slip on magnetohydrodynamics (MHD) boundary layer viscous flow and heat transfer of a nano fluid over a non-linearly-stretching sheet:a numerical study, *Propulsion and Power Research*, Doi.org/10.1016/j.jppr.2018.04.003

Rawat, S. Kapoor, S. and Bhargava, R. (2016). MHD flow and heat transfer of micropolar fluid over a nonlinear stretching sheet with variable micro inertial density, heat flux and chemical reaction in non-Darcy porous medium. *J Appl Fluid Mechanica, 9*(1), 321-331..

Reena and Rana, U. S. (2009). Effect of Dust Particles on rotating micropolar fluid heated from below saturating a porous medium. *Applications and Applied Mathematics: An International Journal. 4*, 189-217.

Sakiadis, B. C. (1961). Boundary layer behaviour on continuous solid surfaces: II The boundary layer on a continuous flat surface. *A.I.Ch.E.J. 7*, 221-225.

Takhar, H. S., Agarwal, R. S. Bhargava, R. and Jain, S. (1998). Mixed convection flow of a micropolar fluid over a stretching sheet. *Heat and mass Transfer, 34*, 213-219.

Waqas, M., Farooq, M., Khan, M.J., Alsaedi, A., Hayat, T. and Yasmeen, T. (2016), Magnetohydrodynamic (MHD) Mixed Convection Flow of Micropolar Liquid Due to Nonlinear Stretched Sheet with Convective Condition, *International Journal of Heat and Mass Transfer,* 102, 766 – 772.

Vajravelu, K. and Nayfey, J. (1993). Convective heat transfer at a stretching sheet. *Acta. Mechanica, 96*, 47-54.

Vajravelu, K. (2001). Viscous flow over a nonlinearly stretching sheet. *Appl. Math. Comput., 124*, 281-288.